International Conference on Space Optics—ICSO 2022

Dubrovnik, Croatia

3–7 October 2022

Edited by Kyriaki Minoglou, Nikos Karafolas, and Bruno Cugny,

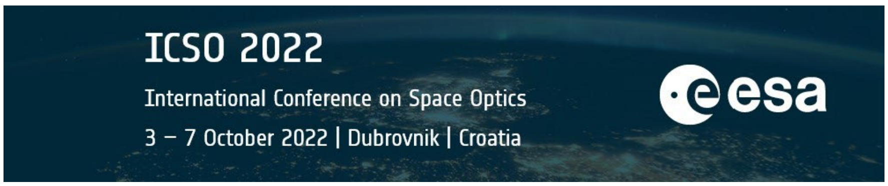

New silicon carbide with light scattering reduction

esa icso proceedings cnes

International Conference on Space Optics — ICSO 2022, edited by Kyriaki Minoglou, Nikos Karafolas, Bruno Cugny, Proc. of SPIE Vol. 12777, 127772Z · © 2023 ESA and CNES · 0277-786X · doi: 10.1117/12.2690320

New silicon carbide with light scattering reduction

M.Ferrato*[a], M.Zerrad[b], M. Fouchier[b], P.Etcheto[c], M.Tatat[c], J.Lavenac*[a]
[a]MERSEN BOOSTEC – ZAE Ceram'Innov Pyrénées, 65460 Bazet, France; [b]Aix Marseille Univ, CNRS, Centrale Marseille, Institut FRESNEL, Marseille, France; [c]CNES, 18 avenue Edouard Belin, 31401 Toulouse Cedex 9, France.

ABSTRACT

Since 1999, MERSEN BOOSTEC designs, manufactures and sells products made of sintered silicon carbide (SiC) mainly for space applications. Improvement of the state of surface of SiC substrates is essential to reduce scattering losses. In collaboration with CNES, a comparative study of microstructural, mechanical, and optical performances of different ceramic processes has been involved to optimized SiC substrates.

Then, the comparative study has been extended to scattering losses in collaboration with the Institut FRESNEL which is expert in light scattering metrology. Comparative measurements on the developed substrates have been performed on Spectrally and Angularly resolved Light Scattering characterisation Apparatus (SALSA).

This communication will present the results of this study which are already very promising for the development of the next generation SiC optics.

Keywords: Silicon carbide, space, optics, scattering light, surface analysis.

1. INTRODUCTION

Due to its high stiffness and thermal stability, Silicon Carbide [1] is used for Space Optics applications but some challenges are still remaining for its optimisation. Whereas it can be polished until very low roughness, its sintered microstructure has residual microstructural defects which can generate some straylight and residual scattered light. This is the reason why SiC deposited by Chemical Vapor Deposition (CVD) on the mirror blank surface could be necessary depending on the objective of the mission.

2. SILICON CARBIDE MANUFACTURING

BOOSTEC® SiC material and process

BOOSTEC® SiC is an exceptional ceramic for SiC hardware for space and ground optics applications widely used since the beginning of 2000's. This is mainly due to cost effective and high-performance property material given on Table 1. BOOSTEC® SiC gives a unique access to large and complex parts by the process described on Figure 1 [2].

First step concerns ready-to-press granule manufacturing by spray drying of a slurry of submicronic, isotropic powders homogenously mixed with organic binders. Second step consists in isostatic pressing under high pressure both to ensure high cohesion and isotropic blank material [3] before green machining which is the next step. Our technology allows access to a wide range of shape and size until 3.5 m by post sintering assembling.

The SiC CVD cladding which is presented here after is dedicated to the mirrors, when necessary. The other technologies are used for manufacturing the mirrors but also the telescopes structures with large size (Table 2).

Table 1. BOOSTEC® SiC properties.

Properties	Typical Values @ 293 K
Density	3.15 $g.cm^{-3}$
Young's modulus	420 GPa
Bending strength / Weibull modulus (coaxial double ring bending test)	400 MPa / 11
Poisson's ratio	0.17
Toughness (K_{1C})	3.5 $MPa.m^{1/2}$
Coefficient of Thermal Expansion (CTE)	$2.2 \cdot 10^{-6}\ K^{-1}$
Thermal Conductivity	180 $W.m^{-1}.K^{-1}$
Electrical conductivity	10^5 Ω.m

*marc.ferrato@mersen.com; phone 00 33 5 62 33 45 04; mersen.com

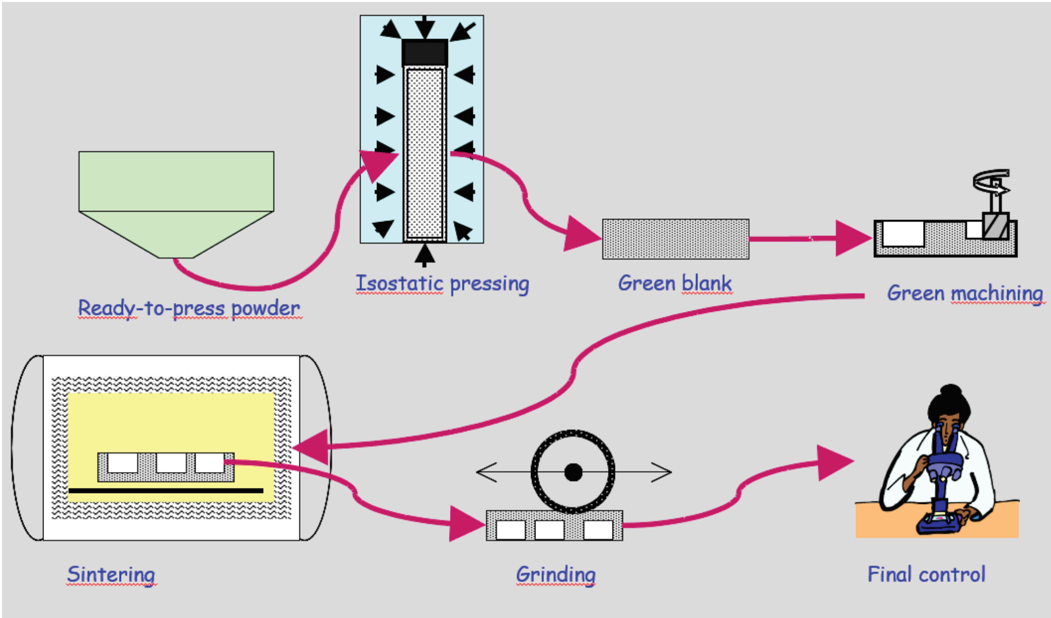

Figure 1: BOOSTEC® SiC process.

Table 2. BOOSTEC® SiC process capability.

	CAPACITY
MONOLITHIC CERAMICS	Ø 1.30m x 0.60m 1.65m x 1.30m x0.60m
CVD SIC COATING	up to Ø 1.50 m
BRAZED SIC/SIC	up to Ø 3.50 m
OPTICAL POLISHING	

	AVAILABLE ASSEMBLIES
OTHER SiC/SiC OR SiC/METAL SOLUTIONS	Epoxy gluing Bolting Shrink fitting

This technology has allowed to manufacture all SiC NIRSPEC instrument for JWST NASA/ESA mission (Figure 2). To decrease scattering light, SiC CVD (Chemical Vapor Deposition) has been deposited on NIRSPEC blank mirror surfaces. This material has been characterized during this study and compared with two other SiC materials (regular BOOSTEC® SiC and HIP SiC (Hot Isostatic Pressing)).

HIP SiC is a new material developed specifically during this study on the basis of SiC BOOSTEC® material.

The objective is to replace a part of SiC CVD business by uncoated SiC material to decrease cost and time to market.

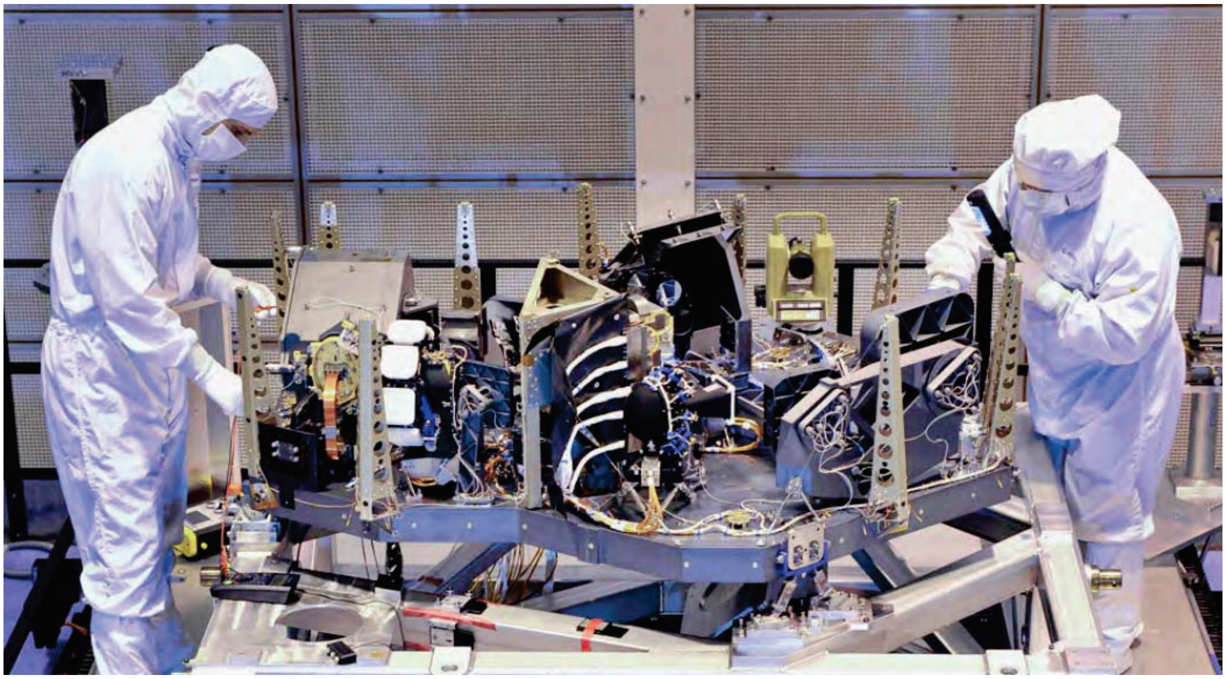

Figure 2. BOOSTEC® SiC NIRSPEC instrument for JWST mission.

NIRSPEC instrument is constituted with more then 40 SiC parts (structural elements like baseplate (1.9 x 1.3 x 0.7 m) and SiC mirrors with CVD coating) produced by MERSEN BOOSTEC. Another mediatic example is all SiC telescope for GAIA mission (Figure 3) which allows exceptional observations due to high precision and stability due to SiC equipment.

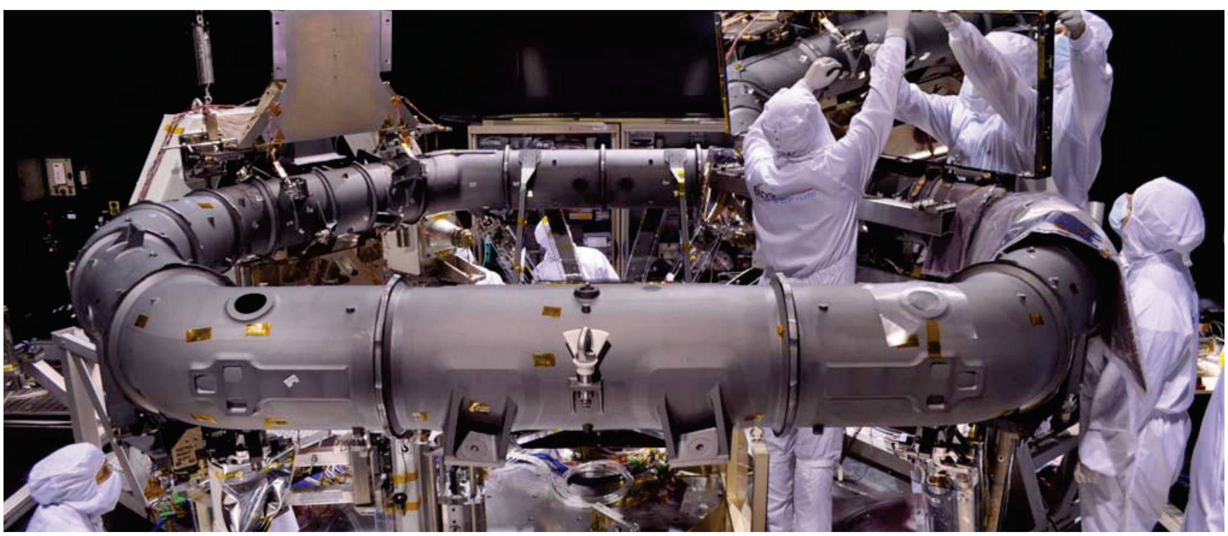

Figure 3. BOOSTEC® SiC GAIA instrument.

3. EXPERIMENTAL DESCRIPTION

Optical bench for characterization (SALSA instrument)

The scattering measurements were performed with the Spectral and Angular Light Scattering characterization Apparatus (SALSA) developed by the Light scattering Group of the Institut Fresnel [4-7].

SALSA is a spectrally and angularly resolved scatterometer, it allows the accurate metrology of BSDF (BRDF & BTDF) patterns over a continuous spectral range from 415 nm to 1650 nm.

A schematical representation of the set-up is given Figure 4. The illumination source is a supercontinuum laser (WL-SC-400-8), 2 tunable volume hologram filters are used to select the illumination wavelength in the visible (LLTF VIS) and near infra-red (LLTF SWIR) ranges. On the detection line, the light collected by the rotating fiber is sent to a second stage of spectral filtering, throught a monochromator (Shamrock) with 2 outputs one for the visible range with a scientific grade CCD camera (Newton CCD) and the second one with an InGaAs, scientific grade (iDus InGaAs). Two additional photodiodes are also used to compensate the variations of the source (Si photodiode; IR PD, InGaAs photodiode).

The ARS (Angle Resolved Scattering) detectivity is achromatic and close to 10-8 sr-1. The spectral resolution is between 0.25 nm in the visible part of the spectrum (415 nm – 950 nm) and 0.75 nm in the infrared part (950 nm – 1650 nm).

It should also be noted that, on its specular configuration, SALSA allows the measurement of specular transmissions up to 14 decades ($T = 10^{-14}$), a performance 6 decades better than the international state of the art. The scatterometer is operational in ISO 6 clean room and is part of the DIFFUSIF platform of Aix Marseille University and the Institut Fresnel.

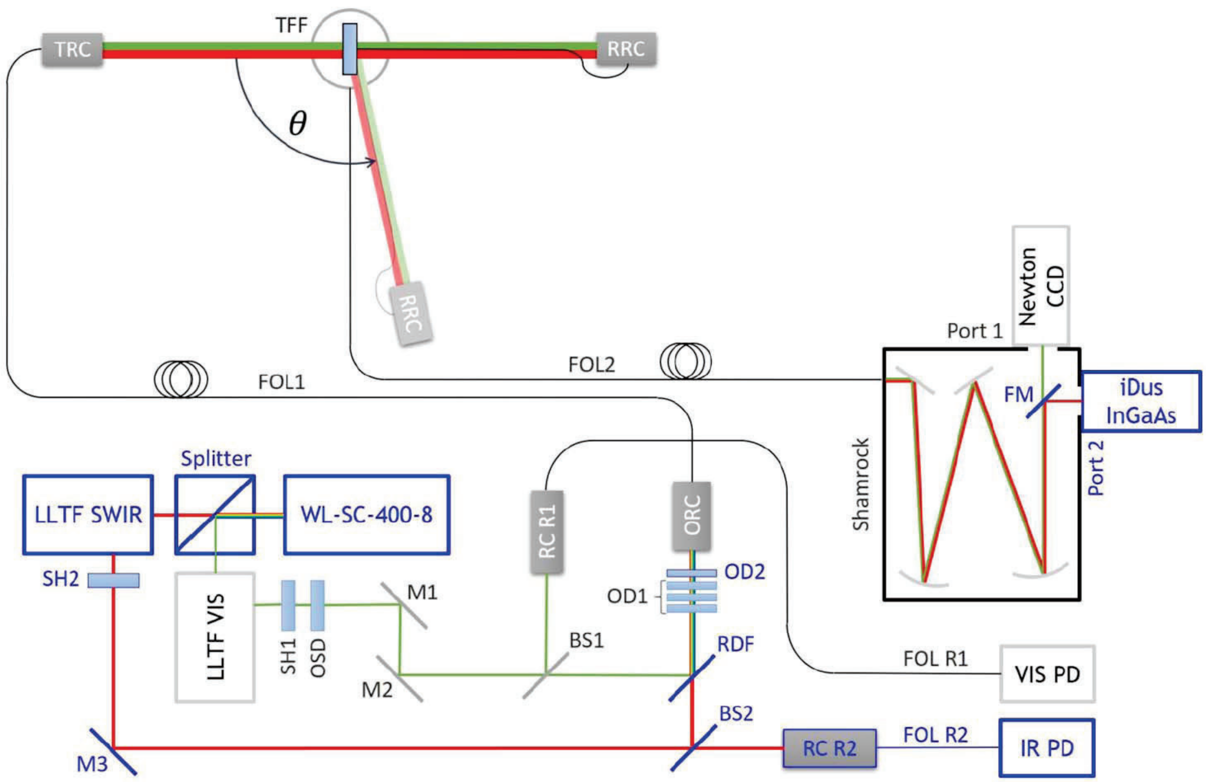

Figure 4 : Schematical representation of the Spectraly and Angularly resolved Light Scattering characterization Apparatus – SALSA -

The calibration is performed with the measurement of a Spectralon © Lambertian sample. The calibration curves are given Figure 5 with the measured signature of the instrument which confirms the detectivity close to 10^{-8}.

The absolute calibration of the scatterometer is achieved using a Spectralon® white diffuse reflectance sample from LABSPHERE measured under normal incidence. The angular variation of the signal, recorded, for instance, at $\lambda = 550$ nm, $\lambda = 800$ nm and $\lambda = 1500$ nm, is shown in Figure 5 in comparison with the theoretical angle resolved scattering (ARS, in sr^{-1}) defined at the same wavelength by:

$$\mathrm{ARS}(\theta,\lambda) = \frac{1}{\pi}\rho(\lambda)\cos\theta \qquad (1)$$

where $\rho(\lambda)$ is the diffuse reflection coefficient of Spectralon® at wavelength λ (ex : ρ=0.9832 at λ =800 nm). The agreement is very satisfactory (note that the result of these calibration measurements is shown with a linear scale).

This demonstrates that our instrument is able to measure high levels of scattered light with great accuracy. To assess its ability to detect very low scattered levels, we also recorded the instrument signature, i.e., the angle resolved signal in the absence of a sample. This floor level is less than 10^{-8} sr^{-1} in the whole angle range between 5° and 175°.

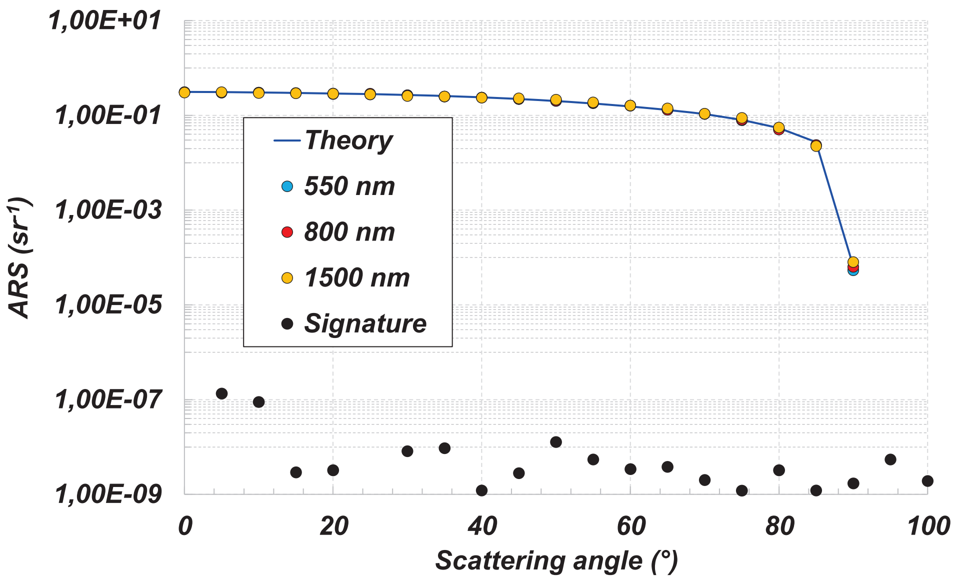

Figure 5 : Signature and calibration of instrument SALSA.

For each measurement, angles are given in reference to the normal direction of the illuminated sample surface, as illustrated Figure 6.

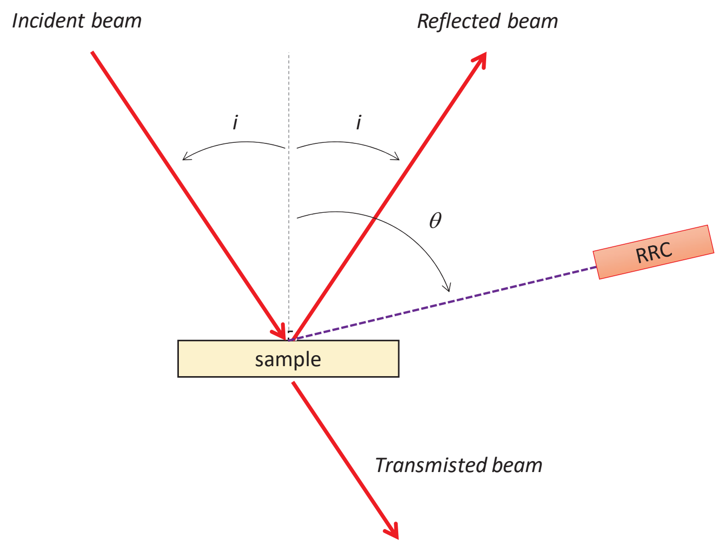

Figure 6. Schematic representation of the angles of analysis, i is for the incidence angle and θ for the scattering angle. They are both given with reference to the normal direction of the illuminated surface.

Experimental methodology

To ensure high sensitive comparison, it was necessary to prepare surface SiC of samples with the same process parameters (same polishing batch, same coating batch and same surface cleaning step). In addition, we defined to reach extremely low and identical roughness below 1 nm rms between intrinsic defects (pores and secondary phases) for all 3 samples (SiC, HIP SiC and SiC CVD). Scattering measurements carried out on SALSA bench have been performed on the same sample before and after optical coating, on the same location (middle of the sample). The objective was to be comparative as finest as possible.

Sample description

3 samples have been selected in a set of several dozen of samples specifically manufactured for this study.

- Sample 1: BOOSTEC® SiC sample manufactured following flow chart on Figure 1.
- Sample 2: HIP SiC material mainly based on BOOSTEC® SiC formulation post-treated at high pressure and temperature.
- Sample 3: SiC CVD which is a CVD coat on BOOSTEC® SiC sample.

Each sample has been polished by free abrasive diamond technic at Boostec in the same batch. Characteristics are given on Table 3. Scattering measurements have been performed in the center of the sample before and after protected silver coat. Protected silver coat has been also performed in the same batch.

Table 3. Main surface parameters for study samples – Area roughness parameters Sq = root mean square height of the surface, Sa = arithmetical mean height of the surface.

Type	Designation	Intrinsic defects surface content (%)	Sq without intrinsic defects (nm)	Sq with intrinsic defects (nm)	Sa without intrinsic defects (nm)	Sa with intrinsic defects (nm)	Density (kg/l)
BOOSTEC® SiC	SiC	5,5	1,4	5,9	0,8	1,7	3,16
SiC HIP	HIP	1,4	1,0	2,0	0,6	0,8	3,20
SiC CVD	CVD	0,1	0,7	0,7	0,5	0,5	3,21

Intrinsic defects are microstructural defects: porosity and/or secondary phases determined by optical microscopy, optical profilometer and Atomic Field Microscopy (AFM).

4. RESULTS

Scatter distribution

BRDF : Three samples representative of the three manufacturing technologies described previously were characterized in terms of optical losses and microstructure. For each of them, the Angle Resolved Scatter (ARS) was measured with an angle of incidence of 2.5 °, with an unpolarized illumination for 3 wavelengths: 550 nm, 800 nm and 1500 nm. The ARS was then converted to Bidirectional Reflection Distribution Function (BRDF) and re-centered for normal incidence. The resulting BRDF is plotted in Figure 7 for uncoated samples, and in Figure 7 for silver-coated samples.

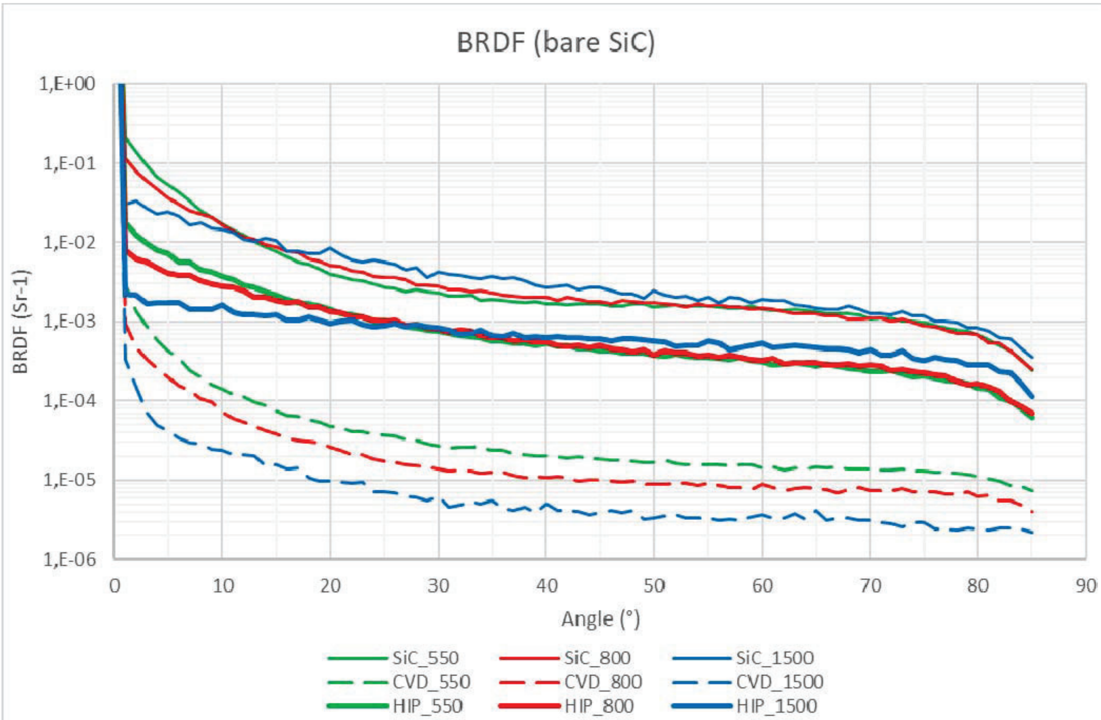

Figure 7 BRDF for bare SiC, CVD and HIP at λ = 550 nm, 800 nm and 1500 nm.

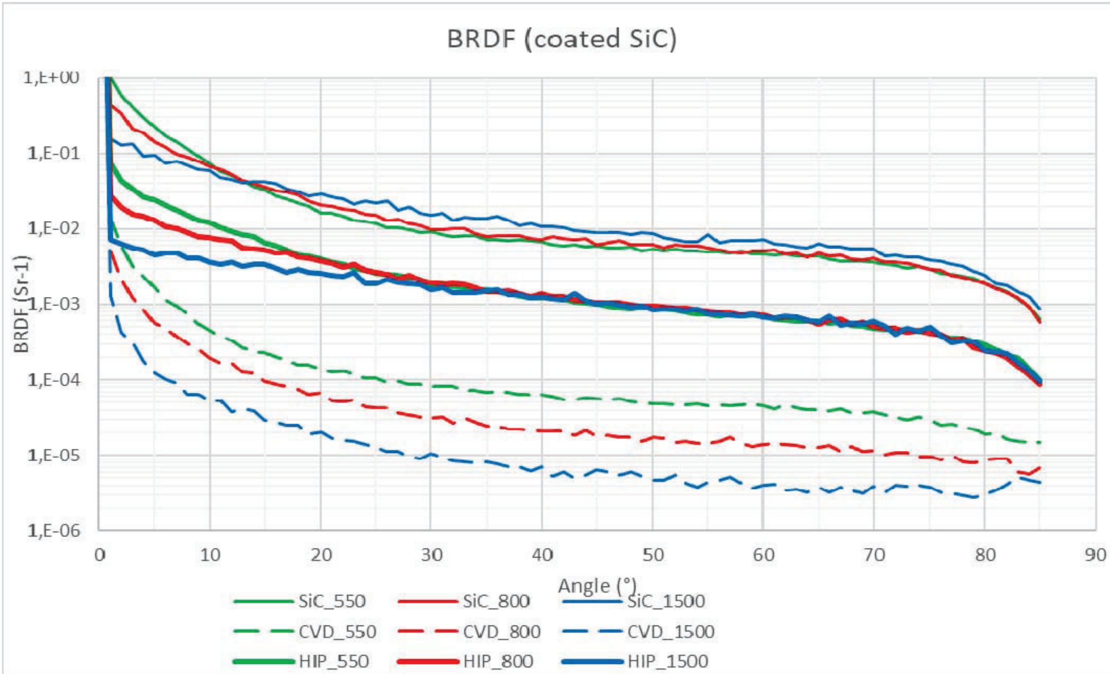

Figure 8. BRDF for silver-coated SiC, CVD and HIP at λ = 550 nm, 800 nm and 1500 nm.

All BRDF curves appear to be valid, well above measurement noise and with a clear cut with the bench signature at 0.5° from specular. The angular distribution of scattered light looks typical of optical smooth surfaces. CVD is strongly dependent on wavelength, while SiC and HIP are wavelength dependent mostly below30°, and much less beyond.

In order to compare the scatter slopes and to fit Harvey-Schack type models, the BRDFs of coated samples were plotted in figure 8 towards "$\beta-\beta_0$", the projected distance to the specular reflection: $\beta-\beta_0$ = sin(scatter angle)-sin(specular angle).

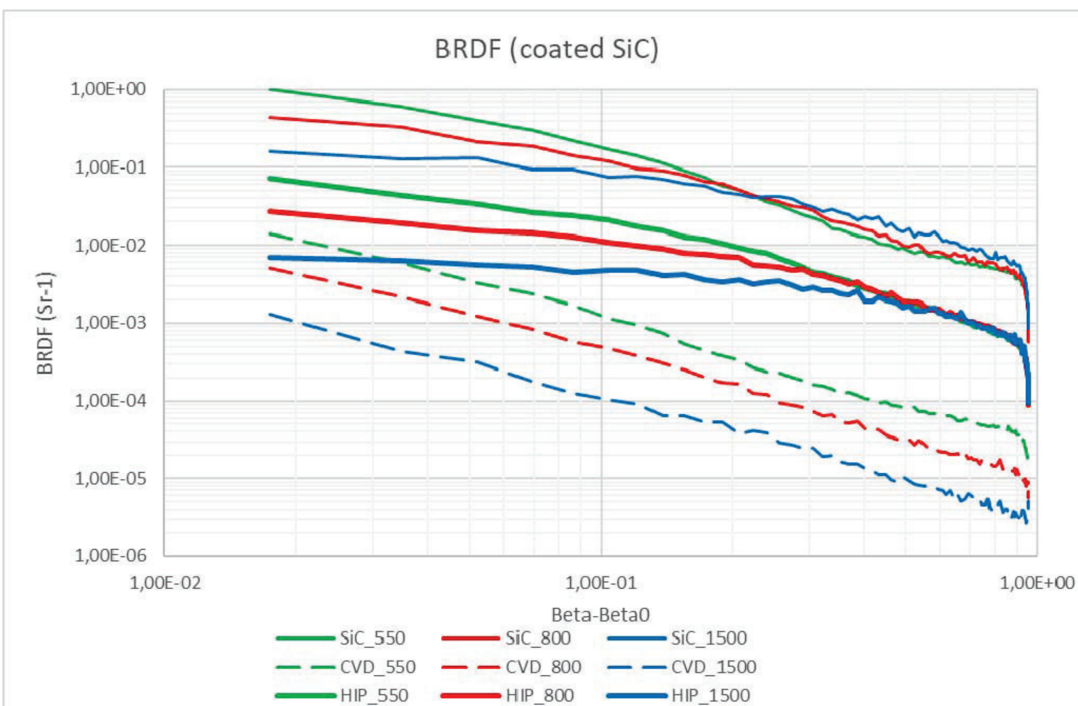

Figure 9. BRDF ($\beta-\beta_0$) for silver-coated SiC, CVD and HIP at λ = 550 nm, 800 nm and 1500 nm

The BRDF of SiC-CVD decreases with the wavelength, with a constant slope: this is typical of scalar scatter by very smooth surfaces, which have a continuous log-normal spectrum of micro-roughness. The BRDF of SiC have a broken slope, which can be described with a composite model. This slope break is due to the dual scatter by polishing micro-roughness and by large porosities. Wide-angle scatter depends little on the wavelength, but near-specular scatter much more. The BRDF of HIP SiC shows the same behavior as the SiC's. It is lower overall, due to improved density, and shows a smaller slope near the specular. This means that the HIP SiC is better than SiC especially at small angles, and is less bad than CVD at lower wavelengths.

Coating effect: the bare and coated samples look roughly the same, except for their overall reflectivity. However this must be closely checked, to assess if the coating affects the surface state, i.e. fills or softens some porosities. For this purpose, the bare SiC BRDF has been scaled-up by the ratio of specular reflectivities for each wavelength (Table 4). The ratio is plotted on Figure 10, depending on the angle:

Table 4. bare SiC and Ag coating specular reflectivity.

Wavelength nm	550	800	1500
R (bare sic)	0,2	0,2	0,18
R (Ag coating)	0,96	0,98	0,975
Ratio	4,80	4,90	5,42

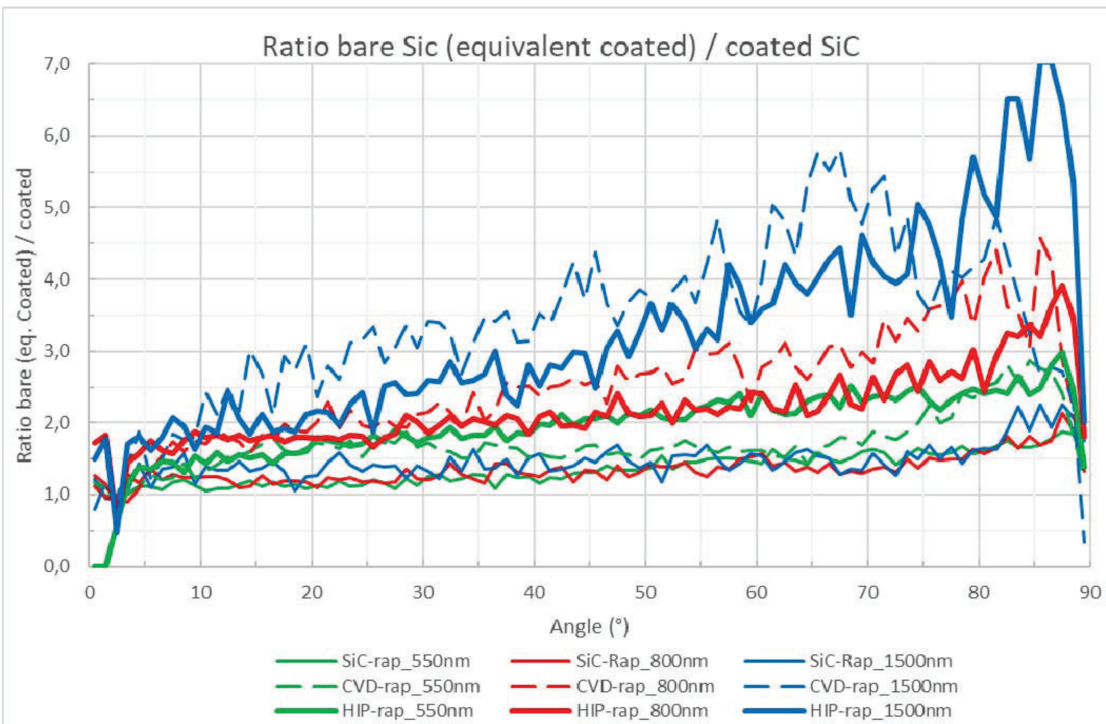

Figure 10. Scaled Bare/coated ratio for SiC, CVD and HIP at λ = 550 nm, 800 nm and 1500 nm.

For common SiC, the ratio is close to 1 at all angles and wavelengths, meaning that the coating has little effect on the SiC relatively large porosities. For SiC-CVD, uncoated samples scatter up to 5 more times in the IR. This is unexpected since the bare CVD is very well polished so the coating should change little. For HIP SiC, the ratio stands between those of SiC and CVD, except at 550 nm where it is higher. We have no explanation yet, unless the bare samples were less well cleaned than the coated ones, which would be much more sensitive for the CVD. Anyways, since the ratio is overall much higher than 1, the main the conclusion is that the results on coated samples are the most relevant, since they are representative of the end-to-end process on user's point of view.

Synthesis of optical properties :

For each SiC and wavelength, we give in Table 5 the most significant features on user's point of view: total hemispherical scatter (albedo or TIS) computed from the BRDF tables, and the BRDF for a small (10°) and a large angle (45°). The TIS is relevant for widely illuminated optics, like a front mirror in Earth observation. Small angles are relevant for in-field of view straylight for moderate aperture mirrors. Large angles are relevant for very wide apertures and for folding mirrors.

Table 5. SiC, CVD and HIP Sic optical performances synthesis.

Type of SiC	**bare SiC**			**bare CVD**			**bare Hip**		
wavelength nm	**550**	**800**	**1500**	**550**	**800**	**1500**	**550**	**800**	**1500**
Total scatter	1,3E-02	1,2E-02	1,3E-02	1,3E-04	6,3E-05	2,2E-05	2,6E-03	2,5E-03	2,2E-03
BRDF (10°)	1,7E-02	1,6E-02	1,4E-02	1,4E-04	7,2E-05	2,4E-05	3,7E-03	2,8E-03	1,6E-03
BRDF (45°)	1,7E-03	1,8E-03	2,8E-03	1,9E-05	1,0E-05	3,9E-06	4,3E-04	5,1E-04	6,2E-04

Type of SiC	**coated SiC**			**coated CVD**			**coated HiP**		
wavelength nm	**550**	**800**	**1500**	**550**	**800**	**1500**	**550**	**800**	**1500**
Total scatter	5,2E-02	4,6E-02	4,9E-02	4,4E-04	1,7E-04	4,8E-05	7,7E-03	6,2E-03	4,5E-03
BRDF (10°)	7,5E-02	6,7E-02	5,9E-02	4,5E-04	2,0E-04	5,3E-05	1,2E-02	7,7E-03	3,6E-03
BRDF (45°)	5,9E-03	6,2E-03	8,8E-03	5,6E-05	1,8E-05	6,4E-06	1,0E-03	1,0E-03	1,0E-03

To outline the improvement of HIP over common SiC, and its limitations compared to CVD, both ratios are provided in Table 6. This might help user's trade-off depending on the mission requirements:

Table 6. Comparison coated HIP vs. SiC and CVD.

Type of SiC	**Ratio**	**Coated SiC/HIP**		**Ratio**	**Coated HIP/CVD**	
wavelength nm	**550**	**800**	**1500**	**550**	**800**	**1500**
Total scatter	6,7	7,4	10,9	17	37	94
BRDF (10°)	6,2	8,6	16,2	27	39	68
BRDF (45°)	5,8	6,0	8,6	18	58	160

Total scatter for HIP is 0.8% (green) to 0.45% (SWIR), that is 6.7 to 11 times better than SiC depending on the wavelength. This is a significant improvement. At small angles, HIP compared even better to SiC, especially in SWIR. This is where HIP appears the most promising. The gain is somewhat less at large angles.

Compared to CVD, HIP is 20 (green) to 100 times (SWIR) worse, since it is less spectrally dependent than CVD. HIP stands no comparison with CVD, especially in the SWIR.

5. CONCLUSION

Optical performances :

HIP-SiC scatters 0.8% (green) to 0.45% (SWIR), which is 6.7 to 11 times better than SiC. Its BRDF at small angles is even better, 16 times better the SiC's in the SWIR. This is where HIP appears the most promising. Yet regarding scatter, HIP cannot compete with CVD, especially in the SWIR. These results are consistent with roughness measurements and with defects cartography by microscope.

Industrial considerations :

From the industrial point of view, HIP SiC requires post treatment which has a cost and delivery impact but not really drastic compared to the pressureless SiC process. On the other hand, the pressure process (HIP) reduces delivery time and cost compared to the CVD SiC process. A trade-off shall be performed case by case depending on the requirements.

Moreover, HIP SiC shows volumic optical properties which simplify the mirror manufacturing process compared to SiC CVD process. It simplifies post finishing steps (grinding, lapping, polishing) and all associated control steps. By decreasing handlings, part safety is improved.

regarding the size limit, due to high pressure and temperature, vessels are not as larger than for the pressureless process (Table 2). 200 mm class SiC HIP mirrors have been manufactured. We are expecting new equipment which will increase capability to half a meter class mirrors.

Possible uses :

These optical performances shall be balanced with the industrial constrains for each type of mission. Within the available size limit, replacing SiC by HIP clearly comes as a cheap but quite significant improvement: it reduces straylight and scatter-induced losses by a factor of 7 to 10. HIP mirrors could be interesting both for Earth observation by Pleïade-size or smaller instruments, and for laser telecommunications. For astronomy however, straylight requirements are generally too hard to dispense with CVD or other very smooth technologies. Finally, HIP might become an alternative to CVD when trading-off between moderate straylight requirements and cost.

ADKNOWLEDGEMENT

This study has been granted by CNES in the frame of R&T programs.

REFERENCES

[1] Bougoin, M., Lavenac, J., « From Herschel to GAIA, 3m-class SiC space optics », Optical Manufacturing and Testing IX, Proceedings of the SPIE, Volume 8126, 8160V-1, 2016

[2] Bougoin, M., Lavenac, J., Pamplona, T., Martin, L., Gimenez, J.-L., Castel, D., Maciaszek, T., « The SiC structure of the Euclid NISP instrument », Proceedings Volume 10562, International Conference on Space Optics — ICSO 2016; 105624J (2017).

[3] M. Bougoin, D. Castel, F. Levallois, “CTE homogeneity, isotropy and reproducibility in large parts made of sintered SiC”, *Proceedings of ICSO 2012 (International Conference on Space Optics)*, Ajaccio, France, Oct. 9-12, 2012

[4] Liukaityte S., Lequime M., Zerrad M., Begou T., and Amra C., “Broadband spectral transmittance measurements of complex thin-film filters with optical densities of up to 12,” Opt. Lett. 40, 3225–3228 (2015).

[5] Lequime M., Liukaityte S., Zerrad M., Amra C., “Ultra-wide-range measurements of thin-film filter optical density over the visible and near-infrared spectrum,” Opt. Express 23, 26863–26878 (2015).

[6] Lequime M., Zerrad M., and Amra C., "Breakthrough spectrophotometric instrument for the ultra-fine characterization of the spectral transmittance of thin-film optical filters," Opt. Express 26, 34236-34249 (2018)

[7] Fouchier M., Zerrad M., Lequime M., Amra. C. Wide-range wavelength and angle resolved light scattering measurement setup. Optics Letters, Optical Society of America - OSA Publishing, 2020, 45 (9), pp.2506-2509.